JOURNAL OF SOLID STATE CHEMISTRY 8, 1–13 (1973)

Crystal Chemistry of Lithium in Octahedrally Coordinated Structures. I. Synthesis of $Ba_8(Me_6Li_2)O_{24}$ (Me = Nb or Ta) and $Ba_{10}(W_6Li_4)O_{30}$. II. The Tetragonal Bronze Phase in the System $BaO–Nb_2O_5–Li_2O$

T. NEGAS, R. S. ROTH, H. S. PARKER, AND W. S. BROWER

National Bureau of Standards, Washington, D.C. 20234

Received November 20, 1972

The preparation, single crystal growth, and crystallographic properties of a close-packed, eight-layer, hexagonal ($a = 5.803$ Å, $c = 19.076$ Å) modification having the stoichiometry $Ba_8Nb_6Li_2O_{24}$ and of a close-packed, ten-layer, hexagonal ($a = 5.760$ Å, $c = 23.742$ Å) phase with $Ba_{10}W_6Li_4O_{30}$ stoichiometry are discussed. The isostructural $Ba_8Ta_6Li_4O_{24}$ form of the eight-layer phase was also prepared ($a = 5.802$ Å, $c = 19.085$ Å). Proposed crystal structures involve the pairing of lithium and metal (Nb, Ta, or W) octahedra to yield face-sharing units. The relationship of this phenomenon to other known close-packed phases containing Li is demonstrated. An investigation of the $Ba_8Nb_6Li_2O_{24}–Ba_{10}W_6Li_4O_{30}$ system is reported.

A tetragonal bronze phase homogeneity region was delimited at 1200°C in the $BaO–Nb_2O_5–Li_2O$ system. A new orthorhombic phase ($a = 10.197$ Å, $b = 14.882$ Å, $c = 7.942$ Å) was prepared with the stoichiometry $Ba_4Li_2Nb_{10}O_{30}$.

Introduction

A voluminous body of literature exists involving the crystal chemistry of mixed metal oxides that consist of a basic structural framework of oxygen octahedra. Within this general classification, the perovskite and tetragonal bronze-type structures have been investigated extensively. The structure-modifying or stabilizing role of Li^+ in these latter compounds is, however, a subject for which little information is available. This paper concerns the preparation and structure of several perovskite-like phases and tetragonal bronzes containing Li^+.

Experimental Procedure

The following starting materials were used for the preparation of specimens:

$BaCO_3$—high purity, spectrographic grade.

Nb_2O_5—high purity. Spectrographic analyses indicated <0.01% Si; 0.001% Ca and Mg with As, Cu, and Ta only questionably present.

$LiNbO_3$ and $LiTaO_3$—high purity. Spectrographic analyses indicated <0.001% Cr, Cu, Fe, K, Mg, Mn, Na, Rb, Si and 0.001–0.01% Al, Ba, Ca, Ni, Sr.

$BaWO_4$—single crystals, grown in this laboratory. Spectrographic analyses indicated <0.001% Ca, Cu, K, Li, Mg, Si and 0.001–0.01% Na.

Li_2WO_4—single crystals, grown in this laboratory. Spectrographic analyses indicated <0.001% Zn, Fe, Pb; <0.002% Al, Mn; <0.01% Nb, Ta; <0.02% Si; <0.1% Na, K.

WO_3—high purity, anhydrous. Spectrographic analysis indicated <0.1% Si; 0.001% B, Ca, Cr, Mg; 0.0001% Cu.

Weighed amounts of the appropriate starting materials were mixed by hand in a boron carbide mortar, packed in gold trays, and calcined in air for 3 days, with periodic remixing, at 1000°C. Portions of the calcined specimens were equilibrated in sealed Pt tubes within a vertical tube resistance-type quench furnace. After sufficient heating periods, the tubes were quenched in water. The furnace used and the methods of temperature control and measurement are described elsewhere (*1*, *2*).

X-ray diffraction powder patterns of specimens were made at room temperature using a high-

Table 1. X-ray Diffraction Powder Data for $Ba_8Nb_6Li_2O_{24}$ and $Ba_8Ta_6Li_2O_{24}$

$Ba_8Nb_6Li_2O_{24}$					$Ba_8Ta_6Li_2O_{24}$			
d_{obs}	d_{calc}	hkℓ[a]	I_{obs}	I_{calc}[b]	d_{obs}	d_{calc}	I_{obs}	I_{calc}[b]
5.029	5.026	100	3	2	-	5.024	-	1
-	4.860	101	-	<1	4.857	4.858	4	4
4.449	4.446	102	4	6	4.440	4.445	4	14
3.945	3.943	103	5	8	3.941	3.943	5	1
3.459	3.459	104	18	22	3.460	3.460	15	19
3.038	3.039	105	94	63	3.038	3.039	90	64
2.902	2.902	110	100	100	2.901	2.900	100	100
2.687	2.687	106	26	28	2.687	2.688	29	32
2.431	2.430	202	6	6	-	2.429	-	1
2.385	2.384	008	9	8	-	2.386	-	1
2.337	2.337	203	11	12	-	2.336	-	1
2.224	2.223	204	16	14	2.223	2.223	12	9
2.099	2.099	205	54	36	2.098	2.098	56	31
1.9721	1.9715	206	22	17	1.9718	1.9714	24	16
1.9533	1.9530	109	5	2	1.9541	1.9538	7	2
1.8426	1.8423	118	3	5	-	1.8426	-	1
1.7834	1.7834	1,0,10	19	7	1.7843	1.7843	21	8
1.7650	1.7648	214	8	6	1.7647	1.7643	4	5
1.7007	1.7005	215	26	19	1.7005	1.7001	35	19
1.6754	1.6753	300	14	16	1.6752	1.6746	18	16
1.6394	1.6393	1,0,11	7	8	1.6402	1.6401	9	8
1.6308	1.6307	216	13	10	1.6306	1.6305	12	12
1.6205	1.6202	209	2	1	1.6208	1.6205	3	1
1.5941	1.5940	1,1,10	3	<1	1.5944	1.5944	5	1
1.5192	1.5194	2,0,10	13	6	1.5199	1.5197	12	6
1.4509	1.4509	220	21	15	1.4503	1.4502	19	13
1.4272	1.4273	2,0,11	9	8	1.4278	1.4277	7	7
1.4146	1.4146	219	3	<1	1.4146	1.4146	3	1
1.3460	1.3460	2,1,10	11	5	1.3460	1.3461	9	5
1.3379	1.3380	314	3	2	1.3374	1.3375	2	2
1.3094	1.3093	315	11	7	1.3091	1.3089	9	7
1.2806	1.2808	2,1,11	5	6	1.2809	1.2809	4	6
1.2766	1.2766	316	5	5	1.2769	1.2763	4	5
1.2394	1.2395	228	4	3	-	1.2393	-	<1
1.2327	1.2329 1.2327	1,0,15 403	3	1	1.2334	1.2335 1.2322	4	1
1.2149	1.2150	404	1	1	-	1.2146	-	<1
1.1934	1.1934	405	7	6	1.1930	1.1930	6	5
1.1684	1.1686	406	2	2	1.1680	1.1682	2	2
1.1252	1.1255	3,1,10	6	2	1.1252	1.1254	6	3
1.1029	1.1037 1.1028	325 1,1,16	8[c]	10	1.1032	1.1033 1.1033	9	10
1.0965	1.0968	410	9	6	1.0961	1.0963	7	6

[a] Indexed on the basis of a hexagonal cell with $\underline{a}$ = 5.8035 ± 0.0004Å, $\underline{c}$ = 19.076 ± 0.002Å for the Nb form and $\underline{a}$ = 5.8016 ± 0.0003Å, $\underline{c}$ = 19.085 ± 0.002Å for the Ta form.

[b] Relative peak height intensities calculated on the basis of an ideal eight-layer stacking sequence with $P6_3mc$ symmetry. Atomic positions used are:

2 Ba in (a), 00z, z ≈ 0;
2 Ba in (b), 1/3 2/3 z, z ≈ 1/8;
2 Ba in (b), 1/3 2/3 z, z ≈ 3/8;
2 Ba in (b), 1/3 2/3 z, z ≈ 3/4;
2 Me (Me = Nb or Ta) in (a), 00z, z ≈ 5/16;
2 Me in (b), 1/3 2/3 z, z ≈ 9/16;
2 Me in (b), 1/3 2/3 z, z ≈ 15/16;
2 Li in (a), 00z, z ≈ 3/16;
6 O in (c), x$\bar{x}$z, x ≈ 1/2, z ≈ 0;
6 O in (c), x$\bar{x}$z, x ≈ 5/6, z ≈ 1/8;
6 O in (c), x$\bar{x}$z, x ≈ 5/6, z ≈ 3/8;
6 O in (c), xxz, x ≈ 5/6, z ≈ 3/4.

[c] broad

angle Geiger counter diffractometer and Ni-filtered Cu radiation. Interplanar *d*-spacings from these patterns were used to compute unit cell dimensions by a least squares refinement computer program. Cell dimensions are estimated to be accurate to within three standard deviations. Single crystals were investigated with an X-ray diffraction precession camera using Mo$K\alpha$ radiation. X-ray diffraction powder pattern intensities were calculated using the program of Smith (*3*).

Experimental Results and Discussion

I. $Ba_8Nb_6Li_2O_{24}$ and $Ba_8Ta_6Li_2O_{24}$ Phases

Kapyshev et al. (*4*) prepared $Ba(Nb_{3/4}Li_{1/4})O_3$ by heating $BaCO_3$, Li_2CO_3, and Nb_2O_5 at 1100°C (1 hr) and 1300°C (1 hr). The phase was reported to be a cubic perovskite ($a = 4.095$ Å) although additional weak diffraction lines suggesting a possible ordering of Nb^{5+} and Li^+ were observed but not indexed. Our preparations of this stoichiometry and the Ta analogue at 1000°C also yielded phases which can be indexed on the basis of a simple cubic perovskite with $a \approx 4.10$ Å. Two weak lines near $d = 3.04$ Å and $d = 2.09$ Å were evident, however, in all of the preparations. These lines are not due to superstructure as their relative intensities increase with increasing heating time. These specimens transform to a new, single phase when heated above 1300°C for several hours. X-ray diffraction powder patterns of this new phase reveal no evidence of the cubic perovskite but contain the two strong lines with *d*-spacings identical with the weak additional lines mentioned above. When reheated at 900°C for 1 week the new modifications do not reverse to the cubic perovskite.

The X-ray diffraction powder patterns of the new phases, given in Table 1, are of excellent quality and were completely and unambiguously indexed on the basis of a hexagonal cell with $a = 5.803$ Å, $c = 19.076$ Å for $Ba_8Nb_6Li_2O_{24}$ and $a = 5.802$ Å, $c = 19.085$ Å for the Ta analogue. Precession data using single crystals of the Nb phase confirmed the apparently large *c*-axis dimension, the *a*-axis dimension, and hexagonal symmetry. The phase was found to melt congruently at 1600 ± 20°C. Clear, anhedral, single crystals (0.1–0.2 mm) are unusually easy to grow either in the solid state at temperatures between 1400–1575°C (24 hr) or by cooling the melt. The crystals proved to have 6/*mmm* Laue symmetry. Zero and upper-level precession photographs show systematic extinctions for $hh2\bar{h}l$: $l = 2n + 1$. Additionally, structural absences $h - k = 3n$ for $l = 2n + 1$ are evident. These absences are consistent with the space groups $P6_3mc$, $P\bar{6}2c$, and $P6_3/mmc$. Based on the volume of the unit cell, the *a* dimension, which is typical of a close packing of Ba and O atoms in a $[BaO_3]$-layer, and assuming an average thickness of 2.35–2.40 Å for one such layer, it appears that the compound is an 8-layer ($8 \times 2.4 = 19.2$ Å $\approx c$) modification.

Crystal growth. A series of crystal growth experiments using the Czochralski technique were made to produce specimens of $Ba_8Nb_6Li_2O_{24}$ large enough for property measurements. A well-insulated Ir crucible was used as the container with RF induction heating because of the relatively high melting point of the phase. In view of the stability of the material during melting point determinations, the atmosphere was not controlled during growth. Losses from the melt due to volatility did not appear significant. In preliminary attempts, growth was initiated on a forked Pt rod. Seeds were cut from the resulting specimens and used in subsequent growth runs. Rotation rates of 20–60 rpm and pulling rates from 5–10 mm/hr were utilized successfully.

Crystals grown by the above technique have a red-brown color which does not disappear after annealing at temperatures of 1000–1400°C. The material is colorless when heated in sealed Pt tubes up to 1600°C. It was observed, however, that in experiments where the Pt tube leaked, particularly near or above 1600°C, quenched specimens had a faint red-orange discoloration. The possibility that the coloration is due to a Li deficiency resulting from volatilization was precluded by the following two experiments. The coloration could not be reproduced by heating compositions specifically formulated to have a slight deficiency in Li. The possibility that the coloration of specimens was due to a contamination by Ir or Pt in an oxidizing atmosphere, therefore, was considered. Chemical analysis of the first crystal pulled from a batch yielded 0.18% Ir. Analysis of a second, somewhat darker red, crystal pulled from the same batch, yielded 0.20% Ir. Thus, it appears that the latter possibility is the most likely cause of the coloration.

$Ba_{10}W_6Li_4O_{30}$ phase. A new phase, $Ba_{10}W_6Li_4O_{30}$, was prepared and found to be stable in the 1000–1400°C range. Its X-ray diffraction powder pattern, given in Table 2 is

Table 2. X-ray Diffraction Powder Data for $Ba_{10}W_6Li_4O_{30}$

d_{obs}	d_{calc}	hkℓ[a]	I_{obs}	I_{calc}[b]
5.940	5.935	004	4	14
4.987	4.989	100	13	14
4.881	4.882	101	6	5
4.602	4.599	102	7	6
4.223	4.220	103	9	12
3.959	3.957	006	6	5
3.821	3.819	104	12	13
3.099	3.100	106	44	35
2.880	2.880	110	100	100
2.805	2.805	107	70	65
2.592	2.591	114	5	8
2.552	2.551	108	2	2
2.494	2.494	200	1	1
2.441	2.441	202	3	2
2.375	2.374	0,0,10	4	4
2.329	2.329	116	8	6
2.300	2.300	204	14	10
2.144	2.144	1,0,10	11	6
2.110	2.110	206	29	20
2.067	2.067	118	1	<1
2.010	2.010	207	45	33
1.9095	1.9094	208	2	2
1.8852	1.8855	210	2	1
1.8617	1.8622	212	1	<1
1.8388	1.8391	1,0,12	1	1
1.8339	1.8342	213	2	2
1.7971	1.7970	214	4	3
1.7196	1.7197	2,0,10	8	4
1.7152	1.7150	1,0,13	23	14
1.7025	1.7021	216	17	10
1.6626	1.6629	300	24	17
1.6478	1.6480	217	35	22
1.6053	1.6056	1,0,14	6	4
1.5499	1.5500	2,0,12	2	<1
1.5336	1.5340 1.5330	219 306	2	2
1.5083	1.5086	1,0,15	1	<1
1.4765	1.4765	2,1,10	8	4
1.4734	1.4735	2,0,13	20	11
1.4613	1.4613	1,1,14	2	1
1.4403	1.4401	220	25	14
1.4023	1.4024	2,0,14	6	4
1.3190	1.3191 1.3190	1,1,16 0,0,18	3	2
1.3117	1.3118	2,1,13	15	9
1.3061	1.3061	316	7	4
1.2810	1.2811	317	13	8
1.2607	1.2609	2,1,14	4	3
1.2313	1.2313	2,2,10	1	1
1.2205	1.2205	404	1	<1
1.1954	1.1954	3,1,10	1	1
1.1894	1.1895	406	2	2
1.1871	1.1873 1.1871	3,0,14 0,0,20	4	3
1.1703	1.1705	407	7	4
1.1028	1.1028 1.1026	3,1,13 1,0,21	8	5
1.0994	1.0994	326	5	4
1.0974	1.0977 1.0975	2,2,14 1,1,20	13	8
1.0886	1.0886	410	8	7
1.0844	1.0844	327	5	5

[a] Indexed on the basis of a hexagonal cell with $\underline{a}$ = 5.7603 ± 0.0003Å and $\underline{c}$ = 23.742 ± 0.002Å.

[b] Relative peak height intensities calculated on the basis of an ideal ten-layer stacking sequence with $P6_3mc$ symmetry. Atomic positions used are:

2 Ba at (b), 1/3 2/3 z, z ≈ 1/20;
2 Ba at (b), 1/3 2/3 z, z ≈ 9/20;
2 Ba at (b), 1/3 2/3 z, z ≈ 3/4;
2 Ba at (a), 00z, z ≈ 3/20;
2 Ba at (a), 00z, z ≈ 7/20;
2 W at (b), 1/3 2/3 z, z ≈ 3/10;
2 W at (b), 1/3 2/3 z, z ≈ 9/10;
2 W at (b), 1/3 2/3 z, z ≈ 6/10;
2 Li at (a), 00z, z ≈ 0;
2 Li at (b), 1/3 2/3 z, z ≈ 2/10;
6 O at (c), xx̄z, x ≈ 1/6, z ≈ 1/4;
6 O at (c), xx̄z, x ≈ 1/6, z ≈ 11/20;
6 O at (c), xx̄z, x ≈ 1/6, z ≈ 19/20;
6 O at (c), xx̄z, x ≈ 1/2, z ≈ 3/20;
6 O at (c), xx̄z, x ≈ 1/2, z ≈ 7/20.

of excellent quality and was indexed completely on the basis of a hexagonal cell with $a = 5.760$ Å, $c = 23.742$ Å. Above ~1400°C quenched specimens showed evidence of melting which is manifested in diffraction patterns by the appearance of new lines corresponding to Ba_3WO_6 and $BaWO_4$. The proportions of these phases increase relative to $Ba_{10}W_6Li_4O_{30}$ when greater amounts of liquid are formed at progressively higher temperatures.

Clear single crystals (0.1 mm), some being hexagonal plates, were grown within sealed Pt tubes heated 24 hr at 1425°C. X-ray precession studies confirmed (and aided) the indexing of the powder pattern. The Laue group, systematic absences, and possible space groups are identical with those of $Ba_8Nb_6Li_2O_{24}$. Similarly, the a and c dimensions and unit cell volume suggest that the repeat unit consists of ten $[BaO_3]$-layers ($10 \times 2.4 = 24$ Å $\approx c$).

Phases in the $Ba_8Nb_6Li_2O_{24}$–$Ba_{10}W_6Li_4O_{30}$ system. It is possible to maintain the perovskite stoichiometry, $Ba_n(Nb_xW_yLi_z)_nO_{3n}$, $(x + y + z = n)$, by varying the proportions of the 8-layer and 10-layer end members. The possibility that hexagonal phases with stacking sequences, other than 8 and 10, dependent on the Nb, W, and Li ratios, therefore, was investigated. Kapyshev et al. (*4*) reported a rhombohedral perovskite ($a = 4.098$ Å, $\alpha = 89°52'$) of stoichiometry $Ba(Nb_{1/3}W_{1/3}Li_{1/3})O_3$ which falls within this series. Weak lines, possibly reflecting an ordering among Nb, W, and Li also were said to occur in their diffraction patterns. At the 1:4 ratio, $Ba(Nb_{1/8}Li_{3/8}W_{1/2})O_3$, a single phase, highly crystalline, cubic perovskite with $a = 8.185$ Å was prepared within the 1200–1400°C range. The doubled a-axis [$a \approx 2(4.1)$ Å] suggests at least a partial ordering wherein the W^{6+} cations are ordered with respect to the position occupied by Nb^{5+} plus Li^+. The formula therefore can be written as $Ba_4(Nb_{1/2}Li_{3/2})W_2O_{12}$. Completely ordered perovskites of this type are also reported by Katz and Ward (*5*) and Blasse (*6*). A detailed

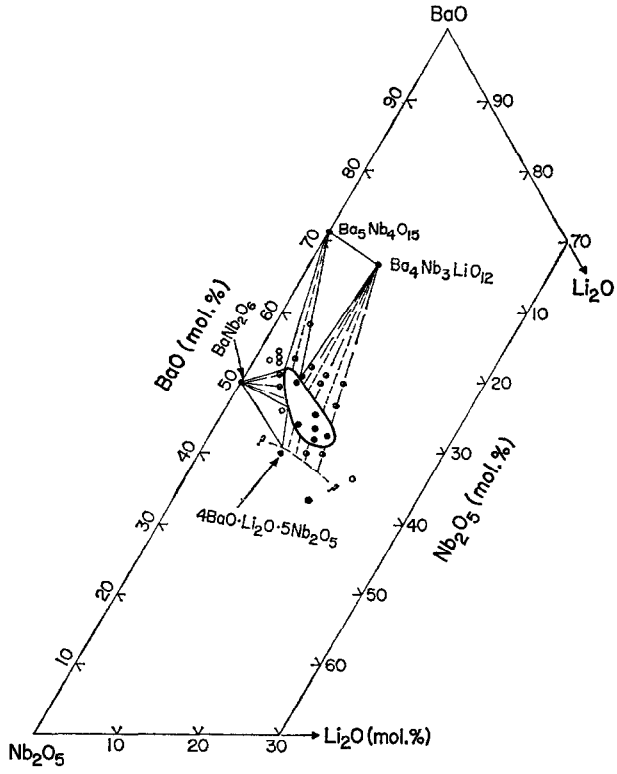

FIG. 1. Phase relations at 1200°C within a portion of the BaO–Nb_2O_5–Li_2O ternary, illustrating the homogeneity region (elliptically shaped area) of tetragonal bronze. Symbols used: ○, three solid phases; ◑, two solid phases; ●, single phase solid; ⊗, unidentified assemblage. The position of boundary curve (?) between the homogeneity region of orthorhombic $Ba_4Li_2Nb_{10}O_{30}$ (see text) and two phase field was not determined.

Table 3. Summary of Experimental Data in the $BaO-Nb_2O_5-Li_2O$ System

Composition (mole %)			Results		
BaO	Nb_2O_5	Li_2O	1200°C	br. Formulation[a]	Other Experiments, Comments
58.33	37.50	4.17	br. + 5H		
54.55	43.18	2.27	br. + 5H + BN		1275°, 18 hr 1325°, 5 hr, no melting, br. + BN $Ba_6(Nb_{9.5}Li_{0.5})O_{30}$ not a br.
53.71	43.57	2.71	br. + 5H + BN		
53.33	45.00	1.67	br. + 5H +BN		
53.33	41.67	5.00	br. + 5H		1325°, 5 hr, no melting
52.87	43.96	3.16	br. + 5H + BN		1325°, 5 hr, no melting
52.17	40.22	7.61	br. + 8H		
51.16	44.77	4.07	br. + BN		
51.06	38.83	10.11	br. + 8H		
51.00	42.00	7.00	br. + 8H		
50.00	43.18	6.82	br. a=12.585±0.001Å c= 4.008±0.001Å	$Li_{0.5}(Ba_{5.5}Li_{0.5})(Nb_{9.5}Li_{0.5})O_{30}$	1325°, 5 hr, no melting
50.00	40.22	9.78	br. + 8H		
50.00	37.50	12.50	br. + 8H		
49.41	45.59	5.00	br. + BN		
46.67	40.00	13.33	br. + 8H		1255°, 1 hr, no melting 1277° and 1300°, 1 hr each, partly melted 1325°, 1 hr, completely melted[b]
46.00	47.00	7.00	br. + BN + X		
45.45	43.18	11.36	br. a=12.557±0.001Å c= 3.996±0.001Å	$Li(Ba_5Li)(Nb_{9.5}Li_{0.5})O_{30}$	1325°, 1 hr, partly melted
44.00	46.00	10.00	br. a=12.504±0.001Å c= 3.992±0.001Å	$Li_{0.48}(Ba_{4.65}Li_{1.35})(Nb_{9.72}Li_{0.28})O_{30}$	

43.40	44.34	12.26	br. $\underline{a}$=12.533±0.001Å $\underline{c}$= 3.983±0.001Å	$Li_{0.94}(Ba_{4.69}Li_{1.31})(Nb_{9.59}Li_{0.41})O_{30}$	
42.42	43.18	14.39	br. $\underline{a}$=12.538±0.001Å $\underline{c}$= 3.980±0.001Å	$Li_{1.34}(Ba_{4.67}Li_{1.33})(Nb_{9.5}Li_{0.5})O_{30}$	1255°, 1277°, 1300°, 1325°, 1 hr each, partly melted[b]
42.00	45.00	13.00	br. $\underline{a}$=12.506±0.001Å $\underline{c}$= 3.976±0.001Å	$Li_{0.93}(Ba_{4.50}Li_{1.50})(Nb_{9.64}Li_{0.36})O_{30}$	
40.00	50.00	10.00	X	$Ba_4Li_2Nb_{10}O_{30}$	1175°, 240 hr and 1225°, 3 hr single phase X 1275° and 1349°, 18 hr, br. + X 1377 and 1390°, 1 hr, partly melted[b]
40.00	47.00	13.00	br. + X		1255°, 1 hr, no melting
40.00	45.00	15.00	br. + X		1277°, 1300°, 1325°, 1 hr each, partly melted[b]
36.36	43.18	20.45	br. + X		1230°, 3 hr, partly melted[b]
33.33	50.00	16.67	LN + unidentified phase(s)		

abbreviations used: br. = tetragonal bronze; 5H = 5-layer, hexagonal, $Ba_5Nb_4O_{15}$;
BN = orthorhombic $BaNb_2O_6$;
8H = 8-layer, hexagonal, $Ba_8Nb_6Li_2O_{24}$;
X = orthorhombic, bronze-like phase, see text;
LN = $LiNbO_3$.

[a] Based on 30 oxygens per tetragonal cell.

[b] Quenched licuid crystallizes to a tetragonal bronze.

listing of such phases is provided by Goodenough and Longo (*7*).

At the 4:1 ratio, $Ba(Nb_{12/21}W_{3/21}Li_{6/21})O_3$, specimens equilibrated within the 1200–1400°C range are not single phase. X-ray diffraction patterns resemble that of a rhombohedrally distorted perovskite structure with sharp superstructure lines plus much weaker lines of an unidentified phase(s). The pattern can be indexed completely only on the basis of a hexagonal cell with $a = 5.798$ Å, $c = 7.129$ Å. The c-axis dimension suggests a three-layer repeat sequence. These data as well as the similarity of corresponding line intensities suggest that the perovskite phase is structurally analogous to the 3-layer perovskites reported by Galasso et al. (*8*, *9*). Efforts were not made to obtain this modification as a single phase.

The powder pattern of $Ba(Nb_{1/3}Li_{1/3}W_{1/3})O_3$ prepared in this laboratory was reconciled with the above data. It is not a single phase rhombohedral perovskite with superstructure as suggested previously (*4*) but consists of a mixture of the 3-layer perovskite plus the cubic perovskite having a doubled a-axis. A complete investigation of this system to define the homogeneity regions of the observed phases was not made.

II. Tetragonal Bronzes in the BaO–Nb_2O_5–Li_2O System

A tetragonal bronze homogeneity field, illustrated in Fig. 1, was delimited for the 1200°C isotherm in this system. Phase equilibria and X-ray diffraction data, summarized for 26 compositions in Table 3, were used to construct Fig. 1. The limited bronze field is elongated, (but not necessarily bisected) along an axis defined by the series $Ba_{6-x}Li_{2x}[Nb_{9.5}Li_{0.5}]O_{30}$. The x parameter varies between approximately 0.3 and 1.4. The end member composition, $x = 0$, on the $BaNb_2O_6$–$Ba_4Nb_3LiO_{12}$ tie line is not single phase. Similarly, the bulk composition $Ba_4Li_2Nb_{10}O_{30}$ does not form a single phase tetragonal bronze (see below). This composition does not melt "congruently" but does appear to fall within the primary crystallization field of tetragonal bronze solid solution. These results are not in agreement with the data of Hirano et al. (*10*) who reported the growth of single crystals of $Ba_4Li_2Nb_{10}O_{30}$ tetragonal bronze from a melt having the same bulk stoichiometry. Although chemical analysis of their crystals were not given, it appears that Hirano et al. grew a Nb-deficient bronze, as suggested in Fig. 1, from the bronze primary phase field. X-ray diffraction precession studies of bronze crystals (see below) confirmed the cell parameters and tetragonal symmetry deduced from powder patterns.

The $Ba_4Li_2Nb_{10}O_{30}$ phase. Below 1275°C, the $Ba_4Li_2Nb_{10}O_{30}$ composition yields material which has a complex X-ray diffraction powder pattern. It was assumed initially that the composition was probably multiphase. Compositions richer in Li_2O gave similar powder patterns but included tetragonal bronze lines. Crystals obtained from the following experiment resolved the complex X-ray data. A composition (~110 g) consisting of 33.71, 18.35, and 43.94 mole% BaO, Li_2O, and Nb_2O_5, respectively, was melted (~1250°C) inductively. An attempt was then made to pull a single crystal of a tetragonal bronze. The resulting product, although apparently homogeneous, was polycrystalline. The crystals were clear, irregular blocks (<1 mm). Precession studies revealed that some of the crystals were a tetragonal bronze phase while the majority were a new phase having orthorhombic symmetry. Powder patterns of the crushed crystals were identical to those described above. The X-ray powder data for the $Ba_4Li_2Nb_{10}O_{30}$ composition were resolved unambiguously with the single crystal data of these orthorhombic crystals. X-ray diffraction data, given in Table 4, were completely indexed on the basis of an orthorhombic cell with $a = 10.197$, $b = 14.882$, and $c = 7.942$ Å. Possible space groups are *Pcmn* (No. 62) and $Pc2_1n$ (No. 33). The unit cell does not appear to represent an orthorhombic distortion of a tetragonal bronze cell. The c parameter is related to that of a bronze structure by $c_{ortho}/2 = c_{bronze}$ (~3.9 Å). Structural details await a single crystal structure determination. Efforts were not made to delimit the homogeneity region of this orthorhombic phase.

Structural Considerations

I. Eight- and Ten-Layer Phases

Although complete single crystal analyses should be initiated to elucidate structural details,* it nevertheless is possible to predict the ideal structures of the 8- and 10-layer phases. The problem is one of finding appropriate

* Single crystals of these phases have been sent to Dr. L. Katz, Univ. of Connecticut and structural studies are in progress.

Table 4. X-ray Diffraction and Crystallographic Data for $Ba_4Li_2Nb_{10}O_{30}$[a]

d_{obs}	d_{calc}	hkℓ[b]	I_{obs}	d_{obs}	d_{calc}	hkℓ[b]	I_{obs}
8.418	8.412	110	6	-	1.8142	502	*
7.443	7.441	020	11	1.8017	1.8025	370	14
5.101	5.099	200	3		1.8009	512	
-	4.461	130	*	-	1.7956	224	*
4.207	4.206	220	4[c]	1.7775	1.7778	460	4
3.971	3.971	002	17	1.7624	1.7626	522	3
-	3.837	012	*	1.7518	1.7517	044	6
3.720	3.720	040	16	1.7478	1.7476	280	14
-	3.700	102	*	-	1.7447	541	*
3.590	3.591	112	8	-	1.7145	304	*
3.504	3.503	022	37	1.7039	1.7038	532	60
3.312	3.314	310	87		1.7032	314	
	3.313	122		1.6998	1.6996	600	47
-	3.245	231	*	1.6837	1.6846	082	40[c]
3.132	3.133	202	53		1.6824	550	
-	3.125	301	*	-	1.6621	182	*
3.100	3.100	032	8[c]	1.6571	1.6569	620	21
3.066	3.066	212	8[c]		1.6567	244	
3.004	3.005	240	61	-	1.6518	054	*
2.966	2.966	132	100	-	1.6517	611	*
2.887	2.887	222	47	-	1.6459	551	*
-	2.881	321	*	1.6415	1.6413	372	53
2.857	2.857	150	41	1.6311	1.6322	190	20
2.804	2.804	330	28		1.6307	542	
2.714	2.715	042	28		1.6305	154	
2.625	2.624	142	5	1.6211	1.6226	462	12
-	2.582	302	*		1.6204	334	
2.546	2.549	400	28	-	1.5993	471	*
	2.544	312		-	1.5985	381	*
2.479	2.480	060	6	1.5754	1.5758	631	4[d]
-	2.446	251	*	-	1.5665	404	*
-	2.423	123	*	-	1.5625	602	*
2.412	2.412	420	18	1.5577	1.5579	414	5
2.396	2.396	242	17		1.5571	344	
-	2.382	052	*	-	1.5501	064	*
2.320	2.319	152	17	1.5459	1.5459	640	3
2.306	2.306	161	4[d]	-	1.5452	561	*
2.290	2.291	332	8	1.5292	1.5291	622	6
2.240	2.239	350	8	-	1.5027	480	*
2.231	2.230	260	12	1.4873	1.4882	0,10,0	16
-	2.180	431	*		1.4870	390	
2.145	2.145	402	8	1.4721	1.4718	570	3
2.121	2.123	412	8	-	1.4511	074	*
	2.121	342		-	1.4510	651	*
2.103	2.103	440	14	-	1.4498	710	*
-	2.089	303	*	-	1.4479	1,10,1	*
2.081	2.081	170	18	1.4405	1.4406	642	6
2.062	2.061	422	8	-	1.4329	701	*
	2.060	162		1.4283	1.4286	2,10,0	6
2.020	2.020	510	3	1.4056	1.4055	482	3
-	2.011	323	*	1.3924	1.3925	392	3
1.9853	1.9856	004	36	1.3120	1.3118	284	4[c]
-	1.9754	501	*	1.2910	1.2912	604	10
-	1.9691	432	*	1.2836	1.2837	742	17
-	1.9681	014	*		1.2836	554	
1.9501	1.9505	352	26	1.2692	1.2690	136	5
	1.9490	104		1.2610	1.2609	194	5
-	1.9447	262	*	1.2428	1.2427	752	4
-	1.9325	114	*	1.2058	1.2059	840	6
-	1.9092	521	*	1.1978	1.1978	822	7
1.8864	1.8863	530	8		1.1976	762	
-	1.8811	451	*	1.1964	1.1964	682	9
1.8603	1.8603	080	5	1.1903	1.1902	394	7
-	1.8502	204	*	1.1824	1.1824	574	5
1.8437	1.8434	172	8	1.1707	1.1709	714	7
	1.8434	034			1.1708	346	
1.8360	1.8361	214	5	1.1596	1.1596	2,10,4	8
-	1.8225	413	*	1.1531	1.1531	2,12,2	11

[a] Prepared in powder form at 1200°C/10 days. See text for the growth of single crystals.

[b] Indexed on the basis of an orthorhombic cell with $\underline{a}$ = 10.197±0.001Å, $\underline{b}$ = 14.882±0.001Å, and $\underline{c}$ = (3.971)(2) = 7.942±0.001Å.

[c] Broad

[d] These are the only lines with ℓ = odd unambiguously present in the powder pattern. They are very strong in single crystal precession photographs.

* Lines which are present in single crystal precession photographs but are either too weak or are masked by other lines in the powder pattern. These are tabulated only up to 2θ = 65°. Possible space groups, Pcmn (No. 62) and $Pc2_1n$ (No. 33).

stacking sequences which conform to symmetry and stoichiometry-imposed requirements. A detailed discussion of the stacking of close-packed units and generated symmetry is provided in the "International Tables for X-ray Crystallography (*11*). Katz and Ward (*5*) discuss some of the more relevant theoretical and experimental aspects of the stacking of close-packed layers.

It is apparent from the respective sets of cell parameters that a stacking of eight and ten close-packed [BaO_3] units are involved in the above phases. These yield cell contents of $Ba_8X_8O_{24}$ ($X_8 = 6Nb + 2Li$) and $Ba_{10}X_{10}O_{30}$ ($X_{10} = 6W + 4Li$), respectively. Furthermore, the X cations must occupy interlayer positions, octahedrally coordinated with oxygen, generated by the stacking order. Sequences of 8 and 10 [BaO_3]-layers cannot be generated such that all layers are of the cubic type (i.e., ABC) as in the perovskite structure and still belong to the possible hexagonal space groups suggested by the X-ray data. Some hexagonal-type stacking (i.e., ABA) must exist to account for both the periodicity and symmetry. Consequently, these phases must contain some oxygen octahedra which are linked by corner sharing within the cubically stacked (c) layers and some by face sharing within the hexagonally stacked (h) layers. It also was assumed that the highly charged 6+ and 5+ cations do not share common octahedral faces. In the close packed, 5-layer, hexagonal structure of Ba_5(Nb or Ta)$_4O_{15}$ (*5*, *12*), for example, the Me^{5+} cations share corners in the c layers but share faces within the h layers with vacant octahedra. The separation of the highly charged cations, therefore, is maximized within this structural framework. Given $6Nb^{5+}$ (or $6Ta^{5+}$) plus $2Li^+$ and $6W^{6+}$ plus $4Li^+$ octahedrally coordinated cations for the 8- and 10-layer phases, respectively, relatively few possible structural arrangements exist that meet all of the above conditions and restrictions. The proposed, ideal structures are illustrated in Fig. 2. Relative X-ray peak height intensity calculations (*3*), given in Tables 1 and 2, are in reasonable agreement with the observed data. Considering the use of ideal (nonrefined) positional parameters in the calculations, the agreement appears good enough to warrant our acceptance of these structural models. If the observed peak height intensities are tabulated in terms of strong-medium-weak nomenclature, the agreement is excellent. Calculations for structures in which the Nb^{5+} (and Ta^{5+}), the W^{6+}, and Li^{1+} were grouped into face-sharing octahedra proved totally unacceptable. Similarly, calculations in which Li^+ was disordered over all possible octahedral sites proved inconsistent with the observed data. Calculated intensities for models in which Li^+ was disordered only

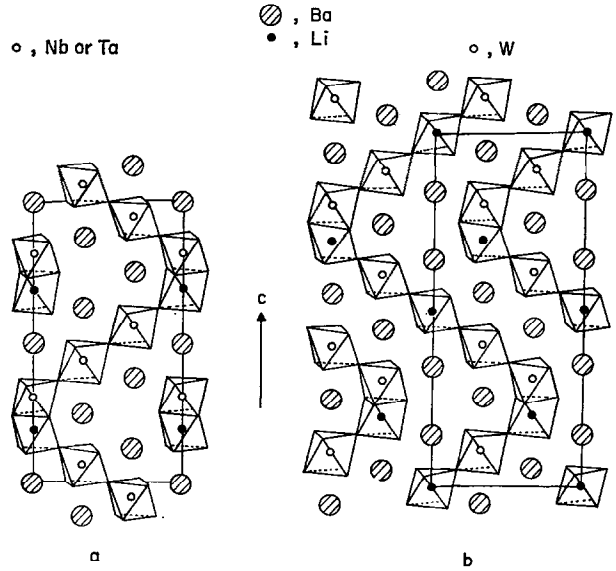

FIG. 2. Proposed structures [(110) view, idealized] of, (a) eight-layer, hexagonal (8H), $Ba_8Me_6Li_2O_{24}$ (Me = Nb or Ta) and, (b) ten-layer, hexagonal (10H), $Ba_{10}W_6Li_4O_{30}$. The octahedral cations in the face-sharing octahedral units are shown ordered in $P6_3mc$ but may be disordered to conform to $P6_3/mmc$ (see text).

within the pairs of face-sharing octahedra showed little difference in comparison with the intensities for the ideal, ordered models. This type of disorder could not be elucidated on the basis of powder data alone. We, therefore, describe the structures in terms of idealized models and suggest (see below) how the possible disorder can be reconciled with the crystallography.

The 8-layer phase has an hccchccc stacking sequence in which pairs of face-sharing octahedra are linked by corners to pairs of octahedra sharing corners. In each pair sharing faces, one octahedron contains Li^+ while the other contains the Me^{5+} cation. The pairing of a Li^+ octahedron with that of another cation to create h-type layers is unusual but, as shall be discussed, not without precedent. Katz and Ward (*5*) propose a theoretical, 8-layer, hexagonal structure with $Ba_8(Me_6Me_2)O_{24}$ stoichiometry while the "International Tables for X-ray Crystallography" (*11*) lists two possible 8-layer sequences with $P6_3/mmc$ symmetry. Our phase appears to be the experimental verification of the Katz and Ward hypothesis and also corresponds to the sequence denoted by the Zhdanov notation |(4)|(4)| in Ref. (*11*). It is noted, however, that if the Li^+ and Me^{5+} cations are ordered in the face-sharing pairs of octahedra as shown, the mirror planes at $z = 1/4$, 3/4 of $P6_3/mmc$ do not exist and the symmetry becomes $P6_3mc$. If a single crystal structure determination reveals disorder within these units, the phase can have the centrosymmetric space group.

The 10-layer phase has an hcccchcccc stacking sequence in which strings of three corner-sharing octahedra are linked by corners to a face-sharing pair. In an ordered arrangement, this pair contains one W^{6+} and one Li^+. Two of the Li cations per cell are accounted for thusly. The remaining two, therefore, must occur within the corner-sharing strings of octahedra. Unless the cations sharing octahedral faces are disordered the symmetry is $P6_3mc$ rather than $P6_3/mmc$. The layer sequence corresponds to the Zhdanov notation |(5)|(5)|, one of the three possible 10-layer sequences with $P6_3/mmc$ symmetry, in Ref. (*11*).

The face-sharing of a Li^+ containing octahedron with one containing another cation is not unknown. The high temperature form of K_2LiAlF_6 (*13*) contains such units. A simple, orderly, structural sequence which illustrates the influence of Li^+ in close-packed structures is shown in Fig. 3. The structures are shown schematically and only include the octahedral cations in the hexagonal (110) view. Low-K_2LiAlF_6 (*14*) is a rhombohedral, 6-layer

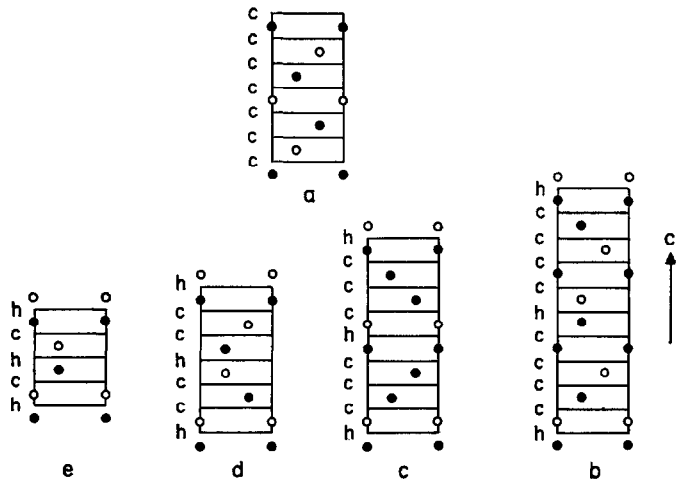

FIG. 3. Close-packed structures (hexagonal (110) view of the octahedral cations) which can be generated by the successive conversion of cubic-type (c) layers to hexagonal-type (h) layers. This results from the pairing of Li^+ and Me^{n+} octahedra. Solid circles are Me^{n+} cations, open circles are Li^+. a. Ordered perovskite, 100% (c) layers, Ba_4ReLiO_6 or K_4AlLiF_6 (low-temperature form). b. Ten-layer, hexagonal, 80% (c) layers, $Ba_{30}W_6Li_4O_{30}$. c. Eight-layer, hexagonal, 75% (c) layers, $Ba_8Nb_6Li_2O_{24}$. d. Six-layer, hexagonal, 66 2/3% (c) layers, K_4AlLiF_6 (high-temperature form). e. Four-layer, hexagonal, 50% (c) layers, oxide or halide not known (see text).

structure in which Li^+ and Al^{3+} octahedra are ordered and share corners. The structure is that of an ordered perovskite in which all layers are of the c-type. A similar oxide compound, referred to a cubic supercell ($a = 8.12 \approx 4.00 \times 2$ Å) is $Ba_2LiRe^{7+}O_6$ (*15*). At ~475°C low-K_2LiAlF_6 transforms to the high form which is an ordered modification of the $BaTiO_3$ structure type (*16*). The high form is a 6-layer sequence but consists of one Al^{3+} octahedron and one Li^+ octahedron each linked by corners to two pairs of octahedra sharing faces. Each face-sharing unit contains one Al^{3+} and one Li^+ octahedron. The transformation to the high form is accomplished by converting every third c-layer of the low form to an h-layer.

In a sequence of all c-layers, if every fourth is converted to an h-layer, an 8-layer modification is generated. Possible oxide stoichiometries which may be accommodated within this structural framework include, $A_8(B_x^nB_y'^m)Li_2O_{24}$, where $x + y = 6$ and $nx + my/6 = 5$ when A is a large alkaline earth. $Ba_8B_6^{5+}Li_2O_{24}$, $y = 0$, is the simplest member. Stoichiometries involving a halogen (X_{24}^{-1}) must conform to $nx + my/6 = 2\,1/3$ when A is a large alakli. A simple stoichiometry, therefore, does not exist. Ordering of three different octahedral cations certainly would be difficult. The Li-rich stoichiometries $A_8^{2+}B_4^{7+}Li_4O_{24}$ and $A_8^{+}B_4^{3+}Li_4X_{24}^{-}$ are also possible but those known, such as $Ba_2Re^{7+}LiO_6$ and K_2LiAlF_6, adopt the ordered perovskite structure type.

If every fifth c-layer in a sequence converts to an h-layer, a 10-layer repeat unit is generated. The simplest oxide stoichiometry which can be accommodated is $A_{10}^{2+}B_6^{6+}Li_4O_{30}$. An alkali–halide analogue as well as oxide or halide formulations richer or poorer in Li necessarily have awkward stoichiometries which involve at least three different octahedral cations.

Longer sequences obviously are possible if the above sequence of conversion of c to h layers is continued. These should be difficult to obtain experimentally as they necessarily require the ordering of Li with at least two other octahedral cations. It is also apparent in Fig. 3 that a 4-layer sequence can be generated by alternating c and h layers. An oxide phase containing Li is not known to have this structure. The simplest required stoichiometries correspond with the known phases $Ba_2Re^{7+}LiO_6$ and K_2LiAlF_6 which adopt the ordered perovskite structure type. It is possible that an ordered 4-layer phase can be prepared if appropriate alkali halides other than KF are chosen as components. The phase $K_4Mn_2F_{12}$ (*17*), however, does have this basic 4-layer framework. If written as $K_4Mn_2\square_2F_{12}$, $\square$ = octahedral vacancy, it is apparent that pairs of face-sharing octahedra are linked by corner sharing. Each pair contains one vacancy and one Mn^{4+}.

Although it is apparent that Li^+ can pair individually with certain 3+, 5+, and 6+ octahedral cations (4+ –Li^+ pairing in oxides is precluded by stoichiometry considerations) in close-packed phases, pairing with a highly charged 7+ cation may be difficult to achieve because of increased electrostatic repulsion. For example, $Ba_2Re^{7+}LiO_6$, prepared at 900°C in air, was found to have the ordered perovskite structure in agreement with Sleight and Ward (*15*). When heated in a sealed Pt tube for several days at temperatures up to 1550°C, transformation to a hexagonal phase did not occur. The phase did not dissociate but did have a darker green coloration which suggests some reduction of the rhenium at the elevated temperatures.

II. Tetragonal Bronzes

The influence of Li on the stability of tetragonal bronzes in the $BaO–Nb_2O_5–Li_2O$ system is reflected by the bulk compositions of single phase materials (Table 3). The unit cell of the familiar tetragonal bronze structure can be described as $A_4A_2'B_4(C_2C_8')O_{30}$. Ideally, the A, A′, and B sites are surrounded by 15, 12, and 9 oxygens, respectively. Atoms in the C and C′ sites are octahedrally coordinated with oxygen. Our bulk, single phase, stoichiometries are written on the basis of 30 oxygen atoms per cell. An oxygen excess was not considered. It is also assumed that all of the C and C′ sites are filled. A deficiency in Nb^{5+}, therefore, is compensated by Li to yield a continuous framework of filled octahedra. Every single phase composition contains a Li excess above that which is required to fill all A + A′ sites (Ba + Li = 6). This suggests that the remainder of the Li must be distributed within the interstitial B sites but the total never attains the possible maximum of four. This remains true even if all excess Li is assumed to occupy the B site. The fact that tetragonal bronzes $Ba_4Li_2Nb_{10}O_{30}$, similar to $Ba_4Na_2Nb_{10}O_{30}$, and $Ba_6(Li_{0.5}Nb_{9.5})O_{30}$, similar to $Ba_6(Ti_2Nb_8)O_{30}$, are not stable suggests, furthermore, that stability is achieved

by the partial substitution of Li in both the octahedral and the B sites. The site occupancy of Li^+ in the orthorhombic, bronze-like, $Ba_4Li_2Nb_{10}O_{30}$ phase is not known.

Conclusions

In this study, it is demonstrated that the Li cation will substitute for octahedrally coordinated cations such as Nb^{5+}, Ta^{5+}, or W^{6+} in either an ordered or disordered arrangement. This type of substitution is not novel but is a phenomenon which has possibilities that are often neglected. It is worth repeating, therefore, that the Li cation may be utilized to lower the average oxidation state of octahedrally coordinated cations in such structure types as perovskite, ilmenite, corundum, the numerous "Mn-oxide" phases, rock salt, tetragonal or hexagonal bronzes, etc.

Further phase equilibria and crystal growth studies concerning the incorporation of Li in many of these structure types are currently under investigation in this laboratory by the present writers and will be reported subsequently.

References

1. T. Negas and R. S. Roth, *J. Solid State Chem.* **1**, 409 (1970).
2. T. Negas and R. S. Roth, *J. Solid State Chem.* **3**, 323 (1971).
3. D. K. Smith (modified by E. H. Evans), A Revised Program for Calculating X-ray Powder Diffraction Patterns, UCRL 50264, Univ. of Cal., Lawrence Radiation Laboratory, Livermore, Cal., 1967.
4. A. G. Kapyshev, V. V. Ivanova, and Yu. N. Venevtsev, *Soviet Physics–Doklady* **11**, 195 (1966).
5. L. Katz and R. Ward, *Inorg. Chem.* **3**, 205 (1964).
6. G. Blasse, *J. Inorg. Nucl. Chem.* **27**, 993 (1965).
7. J. B. Goodenough and J. M. Longo, "Crystallographic and Magnetic Properties of Perovskite and Perovskite Related Compounds," Landolt-Bornstein Tabellen Neue Serie III/4a, Springer-Verlag, Berlin (1970).
8. F. Galasso, J. R. Barrante, and L. Katz, *J. Amer. Chem. Soc.* **83**, 2830 (1961).
9. F. Galasso and J. Pyle, *Inorg. Chem.* **2**, 482 (1963).
10. H. Hirano, H. Takei, and S. Koide, *Japan J. Appl. Phys.* **9**, 580 (1970).
11. "International Tables for X-ray Crystallography," Vol. II, p. 342, Kynoch Press, Birmingham (1959).
12. F. Galasso and L. Katz, *Acta Crystallogr.* **14**, 647 (1961).
13. H. G. F. Winkler, *Acta Crystallogr.* **7**, 33 (1954).
14. H. G. F. Winkler, *Heidelberg Beitr. Min.* **3**, 297 (1952).
15. A. W. Sleight and R. Ward, *J. Amer. Chem. Soc.* **83**, 1088 (1961).
16. R. D. Burbank and H. T. Evans, *Acta Crystallogr.* **1**, 330 (1948).
17. D. Babel, "Structure and Bonding," Vol. 3, Springer-Verlag, New York (1967) pp. 1–88.